Nature Environment and Pollution Technology
An International Quarterly Scientific Journal

p-ISSN: 0972-6268
(Print copies up to 2016)
e-ISSN: 2395-3454

Vol. 24 | No. S1 | pp. 315-330 | 2025

Original Research Paper

https://doi.org/10.46488/NEPT.2025.v24iS1.024

Open Access Journal

Chlorella vulgaris – A Potential Biodiesel Feedstock's Effect on the Performance, Emission and Combustion Phenomenon of a CI Engine with Hydrogen Inductance

S. Pughazhraj[1], D. Balaji[1], V. Hariram[1†], R. Kumaraswamy[1], J. Godwin John[2], P. Naveen[1] and T. S. Ravikumar[1]

[1]Department of Mechanical Engineering, Hindustan Institute of Technology and Science, Padur, Chennai- 603103, Tamil Nadu, India

[2]Department of Mechanical Engineering, Rajalakshmi Institute of Technology, Chennai-600 124, Tamil Nadu, India

†Corresponding author: V. Hariram; connect2hariram@gmail.com

Nat. Env. & Poll. Tech.
Website: www.neptjournal.com

Received: 04-05-2024
Revised: 31-05-2024
Accepted: 17-06-2024

Key Words:
Biodiesel
Fourier transform infrared spectrometry
Chlorella vulgaris
Hydrogen inductance

ABSTRACT

In the modern world, the rise of industrialization and motorization has significantly increased the use of internal combustion engines powered by petroleum products. This has led to the unsustainable exploitation and depletion of petroleum reserves. Consequently, the use of biodiesel-based biofuels, particularly those derived from microorganisms, along with gaseous fuel supplementation in internal combustion engines, has gained prominence. The urgent need to explore alternative fuels for combustion engines has become evident over the past few decades due to the rapid decline in fossil fuel reserves. This study examines the impact of hydrogen induction in the throttle body of a CI engine powered by blends of biodiesel from *Chlorella vulgaris* and mineral diesel in various proportions, without major engine modifications. The research aims to evaluate the performance, combustion, and emission characteristics of the engine when supplemented with hydrogen, biodiesel, and their blend B20. The experiments involve varying fuel compositions and engine operational parameters to assess their influence on efficiency, pollutant emissions, and combustion stability.

INTRODUCTION

The modern era of transportation and other technologies, demands high energy sources that are dependent upon fossil fuels, which are fast depleting and take much time to be produced again, which takes around 150-200 million years. Premiere fossil fuels like coal, products of petroleum, and natural gas are the major sources of energy in transportation, electricity, and much more. These fossil fuels cause harmful pollutants, and atmospheric effects due to carbon emissions (Godwin et al. 2018).

Especially, in internal combustion engines, the emission of harmful pollutants is higher due to the consumption of large amounts of fossil fuels. Researchers have attempted many amicable and efficacious solutions towards reduction in exhaust emission formation and after treatment, thereby replacing the conventional petro-diesel with vegetable/ microorganism-based biofuel in the economically feasible aspects. That produces or emits fewer pollutants in the atmosphere (Hariram et al. 2018). Even though the emission of harmful pollutants produced by biofuel is way less than the traditional diesel fuel or petroleum products. It does not produce the same amount of BTE produced in the conventional, but this can be improved with the addition of hydrogen, which is sent through a manifold with a pilot port into the air inlet. Running Bio-gas biodiesel has resulted in a significant decrement in NOx emissions, Due to alteration in CR and fuel-injection timing CO and HC emissions were reduced. On the addition of nanoparticle CeO_2 and hydrogen to the WCO biodiesel fuel, there is a significant improvement in the BTE and BSFC. Using the response surface method, optimization of hydrogen addition in the various blends of biodiesel according to ASTM D6751, which shows B2O has a significant difference in lower emission and also produces similar efficiency such as BTE, SFC (Subramanian et al. 2020). Using (SME) safflower n Methyl ester, Neem, and Free Methyl can result in the reduction of CO, HC, EGT smoke, vibration, and BTE, when added to the fuel mixture also it increases the BSFC and NOX emission, and also there is a notable increase in consumption of more fuel, but when the combustion chamber is coated with Cr_2O_3, it improves the combustion efficiency. Using CNG with hydrogen has been shown to improve result in heat release rate and reduction in exhaust emission, and brake thermal efficiency such as CO, CO_2, HC (Sarpal et al. 2015)

Oni et al. (2021), did an analysis in which it was seen, that escalated engine loads (i.e., 61%-98%) resulted in higher BTEs with improved engine performance for all fuel blends

in the range of 19–33.9% compared to the Brake Thermal Efficiency (15.1%–19%) of the unblended H-CNG fuel confirming its suitability as an improver to enhance the thermal and combustion efficacy of the compression ignition engine. Additionally, all MB–HCNG fuels exhibited lower exhaust emissions of CO_2, CO, HC, NO_x and O_2 when the unblended H-CNG fuel was used. Suzuki et al. (2015) did an analysis in which it was seen, that we assess how EGR (Exhaust Gas Recirculation) affects performance in light of the rise in NO_x emissions during hydrogen DDF operation. under conditions of 40kW power and 55% H_2 rate. The hydrogen DDF engine's emission level is comparable to that of a heavy-duty diesel engine produced in large quantities when the EGR rate is approximately 20%. Soot emission and pressure variance from cylinder to cylinder are still issues, though.

Raja et al. (2018), did an analysis in which it was seen, that when waste cooking oil (emulsified) was compared to injection timing (advancement), a decrease in smoke emission trend (i.e., 25%) was observed after executing the two alternative control approaches. The merits of lower NO_x emissions from neat Waste Cooking Oil were also attained by the emulsification process. Nevertheless, using emulsified fuels resulted in a slight (i.e., 8%) reduction in BTE, which improved with advancements in injection timing. Therefore, research indicates that the better option is emulsification for running the engine when reducing smoke emissions is the main goal, while advancements in injection timing are recommended for optimal operation when running the engine with pure WCO. Murad et al. (2020), studied the energy contribution of 15 and 38% respectively of hydrogen and ethanol fuel in a dual fuel operation where the brake thermal efficiency increased from 25.2% of neat MO to a maximum of 28.5% and 30% with those fuels, whereas the neat diesel showcased 30.8%. Smoke emission was detailed as 51% under neat diesel operation, whereas the opacity was reduced from 78% (neat MO) to 58% under hydrogen energy sharing of 15% which was better in terms of efficiency. Because of hydrogen induction, it was noted that the NO_x was increased and also it was noted that by adding ethanol and water towards intake the knock limit was extended which increased the BTE. The highest BTE was 30.1% when 5% water was added, and 30.8% when 10% ethanol was injected. Khan et al. (2018), did an analysis in which it was seen, that the results show the lowest HC and CO concentration, greatest BTE, and minimal BSFC, although the NO_x content increased somewhat. It has been discovered that cottonseed biodiesel and its diesel mix closely resembled conventional diesel in terms of combustion properties.

It has shown better combustion efficiency gives higher peak cylinder pressure and does not form any kind of impact danger on the engine structure. However the combustion duration at low engine loads was a bit longer than the conventional fuels with the mixture of rapeseed methyl ester RME, there is a much lower combustion duration at low engine loads. In using waste cooking oil as a biofuel, the effect of different engine parameters and load conditions on the performance and emission of a dual engine has been experimented with. With additional hydrogen gas as gaseous fuel, it improves the increase in BTE and power output but it also increases the emission of pollutants such as CO_2, CO, and NO_X, to reduce the emission, the fuel injection can be turned to reduce emission. Major parameters that can project the characteristics of combustion of WCO are engine speed, H_2 flow rates, and pilot fuel (WCO biodiesel), as the parameter increases a similar increase in BTE and power output can be noticed. During H_2 addition, the oxygen content in the air inlet will be less, which can increase the opacity of the smoke. For every possible parameter experiment, there is an inverse relation shown between BTE and BSFC when there is a rich mixture is combusted, there will be an increase in BTE and a significant decrease in BSFC. Das & Das (2023), worked with waste cooking oil biodiesel and enrichment of hydrogen which improves the thermal efficiency and there is a significant reduction in the emissions when working in CRDI Engine. They introduced iron nanoparticles as a thermal enhancer, limiting their concentration in the biodiesel to 75 ppm. Hydrogen was supplied at a constant rate of 10 LPM through the primary manifold. The addition of iron nanoparticles and hydrogen notably affected nitrogen oxide (NO_x) formation, possibly due to increased oxygen content and nano-additives. Combustion using modified fuel showed decreased levels of smoke, CO, HC, and CO_2 due to more complete combustion. Under maximum engine load, engine efficiency (BTE) increased by approximately 2.6% compared to straight diesel fuel, likely due to enhanced atomization of fuel aided by iron nanoparticles, promoting micro-explosions with hydrogen fuel (Chetia et al. 2024).

Biodiesel derived from microalgae using the transesterification process, which is a process of exchange of organic functional group R" of an ester with R' of alcohol, a single-cylinder diesel engine run by biodiesel as alternative fuel and hydrogen was also added into the air inlet. The engine was operated at different loads with B20 blend, B20 with hydrogen at 2 LPM, B20 blend with hydrogen at 4 LPM, and conventional diesel fuel. Conventional diesel is to compare the results of the biodiesel outcomes. Performance outcomes such as B.TE, SFC, TFC, and indicated power are observed. Combustion characteristics such as in-cylinder pressure and net heat release rate are observed. Emission parameters such as CO, HC, CO_2, NO_X, and opacity are also monitored tabulated, and shown in graphs and discussed.

MATERIALS AND METHODS

This section details the biodiesel source (algae), how it was cultivated, and collected, the oil extraction, the transesterification process, characterization techniques used, and the experimental setup that was utilized for this study.

<fa[_!>ofmp[mih

Chlorella vulgaris can grow and thrive in its suitable environment. Temperature, pH, light intensity, and carbon dioxide concentration are parameters that can be calibrated to grow the algae. It was noted from the literature that *Chlorella* species produce more lipids than a mixture of lipids produced in photoautotrophic and heterotrophic cultures. *Chlorella vulgaris* was noted to grow well in temperatures ranging from 20°C to 30°C. pH emerges as the conductor in algal growth and also it was seen that *Chlorella vulgaris* thrives in slightly alkaline waters, with pH levels maintained between 6.5 and 9.0. Providing CO_2 to the Algae utilizes them for chlorophyll, which also indulges in growth rate and biomass yield. In the Bold Basal medium, the algae were grown using the nutrients nitrogen and phosphorous (in the form of ammonium nitrate and potassium phosphate) which acted as the catalyst for cellular proliferation and enhanced the algal growth. It was noted that the biomass yield was ranging from 0.5 to 2 g/L/day. The microscopic view of chlorella vulgaris is shown in Fig. 1A.

Bdg[mb>iff_]mih

To collect the algal biomass, the centrifugation method was used since separating the cells developed in the aqueous medium can be leveraged efficiently using centrifugal force. Later this stage the biomass was filtered using porous media to drain the aqueous medium from the collected biomass. This filtration will be the parameter that decides the flexibility and scalability of biomass concentration. The flocculation process was also deemed necessary to aggregate larger biomass and its recovery. The collected biomass was then dried for further process Oil Extraction.

Bio-Oil Extraction

To extract oil from the algal biomass, a Soxhlet extractor was used. The procedure was to put the dried algal biomass inside a filter paper thimble and then put the filter paper into a glass cylinder that had an intake tube and a siphon tube attached to it. A water condenser was fastened to the cylinder's top. The setup was then placed into the neck of a flask with a circular bottom that would hold the solvent after it had been heated. The solvent's vapors rise through the inlet tube and into the cylinder as it is heated, condensing will occur at the condenser. The dried mass interacted with the condensed solvent and was dissolved as a result. The solution ensured a steady supply of solvent vapors inside the cylinder by flowing back into the flask whenever it reached the top of the siphon tube. After the extraction process, the heating was stopped and the extracted oil was separated from the solvent by distilling the flask's solution. The effective extraction of algal oil from intricate mixtures is done through this process which takes 5 hours. The collected oil was then evaporated using a rotary evaporator to obtain the microalgae

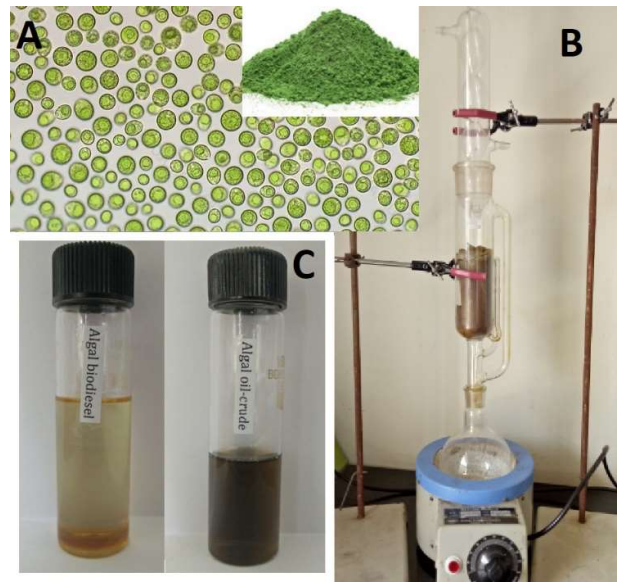

Fig. 1: Biodiesel from *Chlorella vulgaris* Microalgae – Microscopic view (A), Soxhlet Bio-oil Extraction (B) and Extracted Bio-oil and Biodiesel (C).

oil (Godwin et al. 2017) as shown in Fig. 1.

Oh[hmm_lcc][nih

Preparation of biodiesel from *Chlorella vulgaris* Microalgae by single-stage esterification using Potassium hydroxide (KOH) as a catalytic agent and methanol (CH_3OH) as base solvent. The chemical reaction disintegrates the crude algal bio-oil into biodiesel and glycerol, the by-product. The procedural steps involved in the transesterification process in forming the potassium methoxide solution and disintegration process are followed below.

The microalgae extract was taken in a container and the transesterification procedure was carried out where the content was 1000 mL. Laboratory use of methanol was taken in the measured beaker. Potassium hydroxide (KOH) and alcohol were mixed properly by stirring until the KOH was dissolved. The extract content of microalgae taken for the study was kept in a container and was mechanically stirred while heating. When the temperature achieved 60°C, the methoxide solution was poured inside the contained and the stirring was continued until proper dissolvent occurred, during this entire procedure the speed of the stirrer was kept minimal. Past this stage, the container is closed airtight and the solution was stirred at higher speeds (say 720 rpm). The temperature should be maintained at 60°C during the entire process since beyond that temperature methanol may evaporate (Hariram et al. 2017). After two hours the solution should be transferred to a separate glass container which will be kept idle for 24 hours, during which the separation of glycerol and biodiesel occurs. In the upper portion of the container is the biodiesel which will be collected after removing glycerol from the container. The cleaning procedure is followed until the glycerol is completely removed from the biodiesel. After this procedure, the biodiesel will be heated to 100°C so that the remaining water present in the biodiesel is evaporated and the result of this procedure will be the microalgae biodiesel that is used for this study.

Fiolc_l!Oh[hmilg!Dh`l[-l_^!Np_]nlig _nls

Chlorella vulgaris algae were used as a source to produce the biodiesel for which the transmittance was analyzed through the Fourier transform infrared spectroscopy. For analyzing this study Attenuated Total Reflectance Fourier Transform Infra-Red Spectrometer. The chlorella vulgaris biodiesel sample was used in the instrument to study the transmittance of the sample through internal reflection. A single reflection module was used in this study analysis, where an infrared beam will pass through the biodiesel sample which produces a vibration signal (transmittance). During this process, the angle of incidence will be produced while the internal reflection occurs. The instrument used has a range of 450 to 4000 cm^{-1}, it also has a resolution of 2 cm^{-1}. Based on the one mL of sample biodiesel that is kept over the crystal upon passing the infrared will share the signals through evanescent waves (Tan et al. 2023).

G[nb>blig [nial[pbs-M[mhNp_]nlig _nl!(G>MN)!

To verify the presence of fatty acid methyl esters in the biodiesel produced from chlorella vulgaris oil. The instrument used is a single quadrupole mass spectrometer which is along with a gas chromatography system. An SSL injector and capillary columns with a 7500:1 inlet split ratio were installed in the GC system. The GC system has a 450°C oven temperature limit. In the chemical and electron impact ionization modes, a pre-heated monolithic hyperbolic quadrupole mass filter was utilized. There was a range of 106°C to 200°C for the quadruple temperature and 150°C to 350°C for the ion source temperature.

@xp_lcg _hn[f!O_mlN_nop!

The specifications of the engine used are detailed in Table 1 which is a single-cylinder diesel engine. The engine test bed that was used to operate and test the fuel efficiency and the instruments used can be seen in Fig. 2. The measuring parameter, accuracy, range, and uncertainty of the measuring devices used such as Smoke meter, smoke analyzer, tachometer, and the dynamometer are also mentioned in Table 2.

Hs^lia_h!Dh^o]n[h]_!dh!O_m@hadh_

Table 1: Test Engine Specs.

Product	One-cylinder four stroke Diesel engine
Make	Kirloskar, Model TV1x
Stroke	87.5 mm
Bore	110 mm
Rated Power and speed	5.2 kW and 1500 rpm
Compression ratio/ Engine capacity	17.5/661 cc
Cooling arrangement	Water cooling
Piezo sensor	Range 5000 PSI, with low noise cable
Dynamometer	Type eddy current, water cooled
Calorimeter	Type Pipe in pipe
Crank angle sensor	Resolution 1 Deg, Speed 5500 RPM
Propeller shaft	With universal joints
Load indicator	Digital, Range 0-50 kg, Supply 230VAC
Fuel tank	Capacity 15 lit with glass fuel metering column
Load sensor	Load cell, type strain gauge, range 0-50 kg
Air box	M S fabricated with orifice meter and manometer.

Table 2: Emission Analyser Specification.

Instrument	Measuring parameter	Accuracy	Range	Uncertainty (%)
Tachometer	Speed	± 1 rpm	450–6500 rpm	0.22
AVL	NO_x	± 12 ppm	0–6000 ppm	0.24
	CO	± 0.02 %	0–16 % vol	0.14
	HC	± 10 ppm	0–3000 ppm	0.25
	CO_2	± 0.01 %	0–22 % vol	0.22
Smoke meter(AVL)	Smoke opacity	± 1 %	0–100 %	1.2

Comprising the gas cylinder & valve with high pressure, the regulator is stated as the hydrogen supply system which was connected with the engine inlet manifold which is in contact with the flowmeter (utilized to see visually the hydrogen supply from the tank to the engine). The pressure regulator used in the system will reduce the atmospheric pressure value which will be passed through the flame arrester-trap setup through the H_2 flow meter. H_2 flow meter along with a controller is utilized to measure and control the flow rate of hydrogen. The Injection system used here is electronically actuated which will inject microalgae biodiesel at the intake manifold. The injection system comprises a control unit and electronic injector, it can be seen that a microcontroller which is connected to a personal computer controls the amount of microalgae biodiesel injection. Considering the engine speed, the injection strategy for algal biodiesel was calculated while the injection was done at the air intake procedure (Gultekin et al. 2023).

The microalgae biodiesel is sent through the fuel injection system to the engine combustion chamber with hydrogen and air mixture inlet. Initially, the air and hydrogen mixture is allowed to be atomized in the combustion chamber of the diesel engine during 1st stroke of the cycle and allowed to pre-heat in the cylinder during the 2nd stroke of the cycle. Biodiesel is sprayed with the help of a fuel injection system into the cylinder and allowed to combust during the 3rd stroke, and at the final step, exhaust gas is sent out. During the four strokes of the cycle, the air inlet temperature, inlet pressure, hydrogen inlet pressure, flow rate, and the amount of fuel flow are all collected using sensors that are placed and monitored with the help of the computer monitoring the engine setup test rig. The temperature of the fuel flow during

Fig. 2: The engine test rig.

the fuel injection will be observed, and the peak pressure that occurred during the 3rd stroke can be monitored. During the 4th stroke, air exhaust outlet temperature, pressure, pollutant content, and other parameters can be observed to study the combustion behavior of the diesel engine. Using a smoke meter and smoke analyzer the CO, HC, NO_x, CO_2, and opacity of the engine can also be surveyed.

Engine outputs such as brake power, brake thermal efficiency, specific fuel consumption, and total fuel consumption will be derived with the help of the dynamometer and engine soft software to determine the characteristics of the performance behavior of the engine. Single-cylinder Diesel engine setup with Dynamometer and smoke analyzer setup during experiment with Biodiesel B20 blend mixture using Kirloskar, Model TV1, Type 1 cylinder, 4 stroke Diesel, water-cooled, power 5.2 kW at 1500 rpm, stroke 110 mm, bore 87.5 mm. 661 cc, CR 17.5. The performance testing of internal combustion engines, medium and small motors, car transmission components, gas turbines, water turbines, engineering machinery, and oil drilling can all be done with an eddy current dynamometer. This experiment is used to analyze the performance characteristics of the engine by inducing load on the shaft of the engine output and observing the other outputs.

Fo_f!Kip_lnc_m

The fuels used in the diesel engine were checked for their properties to verify with the standard operating values and it detailed closer values as shown in Table 3.

RESULTS AND DISCUSSION

The results determined by the analysis are discussed in this section briefly where the FTIR, GCMS, performance, and emission characteristics.

Fi olc_l!Ol[hmilg !Dl`l[-R_^!Np_]rli nhips

The stretched bending values range from 500 to 3000 cm^{-1} in the *Chlorella vulgaris* FTIR spectrum as detailed in Fig. 3. The conversion of biodiesel of *Chlorella vulgaris* is confirmed through the highest peak (the vibration stretch) shown in FTIR analysis at 1741 cm^{-1}. The hydrocarbon presence in the sample is confirmed through the stretches from 1460 to 1019 cm^{-1}. A very strong signal was seen at stretch 2923 cm^{-1}, a signal somewhat strong was seen at stretch 2853 cm^{-1} and there is a signal which was weak seen at stretch 3008 cm^{-1}, these signals detail and verify the biodiesel conversion. It can also be noted that there is

Table 3: Properties of biodiesel, hydrogen and diesel.

Properties	Unit	*Chlorella vulgaris* Biodiesel	.	Diesel	ASTM biodiesel standard
Density	Kg/m^3	864	0.0881	838	ASTM D240
Viscosity (at 40° C)	mm^2/s	5.2	-	1.9-4.1	ASTM D445
Calorific value	MJ/kg	41.0	119.3	43.8	ASTM D240
Cloud Point	°C	7	-	-15 to 5	ASTM D2500
Pour point	°C	-6	-	-35 to -15	ASTM D2500
Flash Point	°C	115	-	75	ASTM D93
Solidification Point	°C	-12	-	-50 to 10	-
Acid value	Mg KOH/g	0.374	-	0.5 max	-
H/C ratio	-	1.81	-	1.81	-

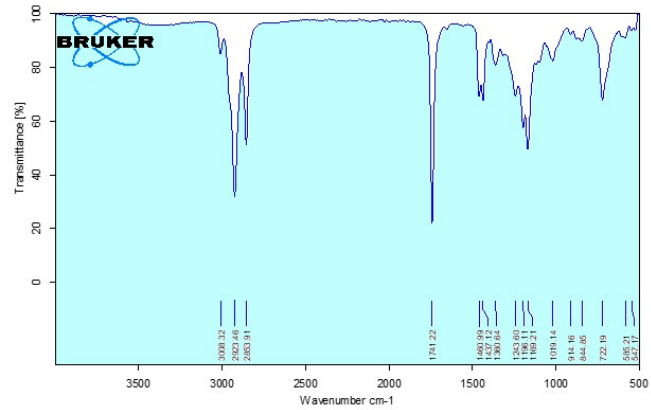

Fig. 3: FTIR Transmittance of *Chlorella vulgaris* biodiesel

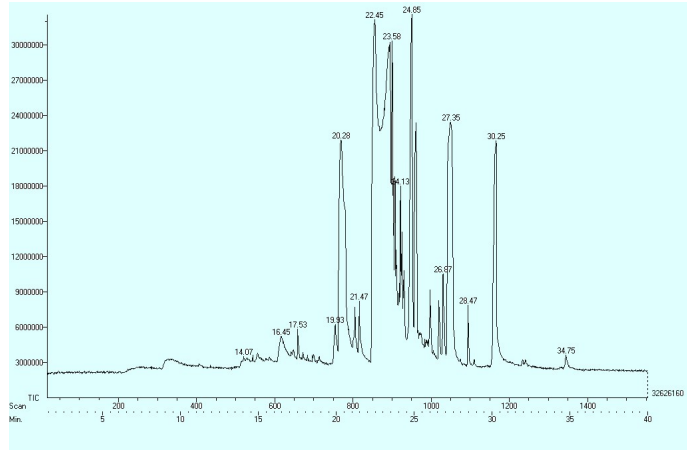

Fig. 4: GCMS spectrum of Biodiesel from *Chlorella vulgaris*.

no trace of stretches between 1741 and 2853 cm^{-1} which is obtained through the single-stage transesterification. Various weak signals were seen near 844, 914, and 1437 cm^{-1} which informs that the carboxylic group is present.

The presence of these distinctive long-chain fatty acid methyl ester (FAME) molecules indicates that these functional groups form the biodiesel.

G[nt>bli g [ni al[pbs-M[mtNp_]nli g _ds

An esterified biodiesel sample was subjected to Gas Chromatography-Mass Spectrometer analysis to determine the existence of different FAMEs and to assess the effectiveness of the process (transesterification). As seen in Fig. 4, the biodiesel's mass chromatogram examined the presence of nine distinct FAMEs at retention times (RT) ranging from 14.07 to 34.75 minutes. Many FAME mass fragmentation patterns demonstrate the loss of carbo-methoxy-ions as a result of β cleavage.

A handful of the mass fragmentation patterns also showed multiple profusions, which could be the result of the group (methoxy) being lost and the hydrogen and carbon atoms being rearranged during the process (transesterification). The hydrogen ion in the carbonyl group rearranges and reorganizes at RT 22.45 min, resulting in the existence of fatty acids (unsaturated) such as 14, 17-Octadecadienoic acid methyl ester (Reang et al. 2020). There were various FAMEs found in the sample analyzed as shown in Table 4.

Table 4: Fatty acid methyl ester with respect to retention time.

S.No.	FAME	Retention Time (RT)
1.	9-hexadecenoic acid methyl ester	19.93
2.	hexadecanoic acid methyl ester	20.28
3.	heptadecanoic acid methyl ester	21.47
4.	14, 17-octadecadienoic acid methyl ester	22.45
5.	eicosanoic acid methyl ester	24.85
6.	13-docosenoic acid methyl ester	26.87
7.	docosanoic acid methyl ester	27.35
8.	tricosanoic acid methyl ester	28.47
9.	tetracosanoic acid methyl ester	30.25

K_l`i lg [h]_!>b[l[]n_lcmc]m

This section details the performance of the hydrogen-inducted fuel (microalgae biodiesel) in the diesel engine. The characteristics of performance that are studied here are indicated power, brake thermal efficiency, friction power, indicated thermal efficiency, specific fuel consumption, and total fuel consumption.

Fig. 5 represents Brake power (BP) vs Indicated power (IP) for the study Engine. The IP varies along the BP, it shows that the diesel has the highest point at 4.92 kW (100% load) at higher load which is 7.22 kW brake power, B20 blend at 7.27 kW, H_2 at 2 LPM 7.39 kW and 4 LPM at 7.45 kW. Where the hydrogen with b20 blend shows higher indicated power with respect to brake power due to the higher combustible nature of hydrogen, it shows higher indicated power produced when the rate of hydrogen flow is increased, and the IP increases also when the rpm increases (Rajak et al. 2022).

Fig. 6 represents Brake power (BP) vs friction power (FP) for the taken study Engine. The FP varies along the BP, it shows that the diesel has the highest point at 2.29 kW at higher load which is 4.92 kW brake power (50% load), B20 blend at 2.38 kW, H_2 at 2 LPM 2.48 kW and 4 LPM at 2.54 kW. Where the b20 blend shows higher friction power with respect to brake power because of higher oxygen availability existing in the fuel B20 blend which enhanced the rate of combustion. Though the O_2 percentage in the biodiesel

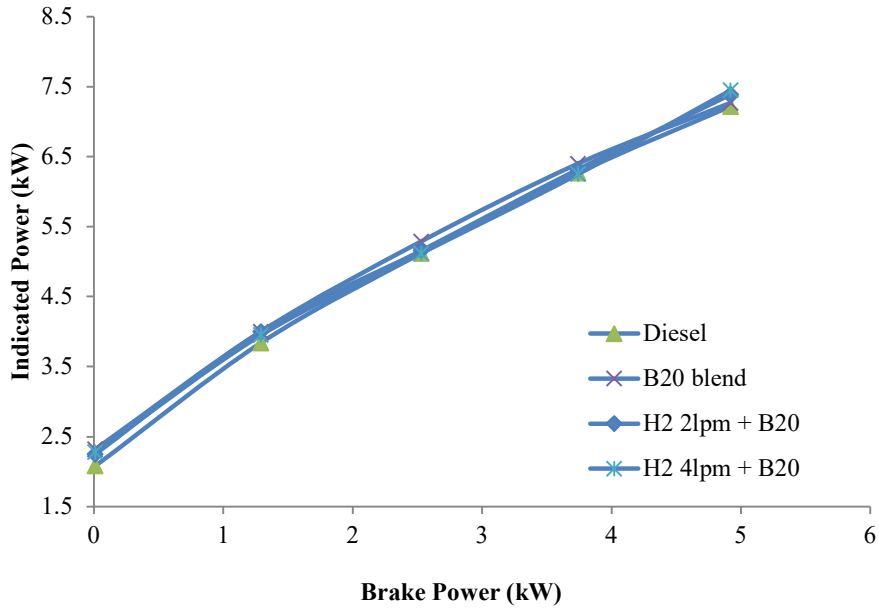

Fig. 5: Variation in Indicated Power.

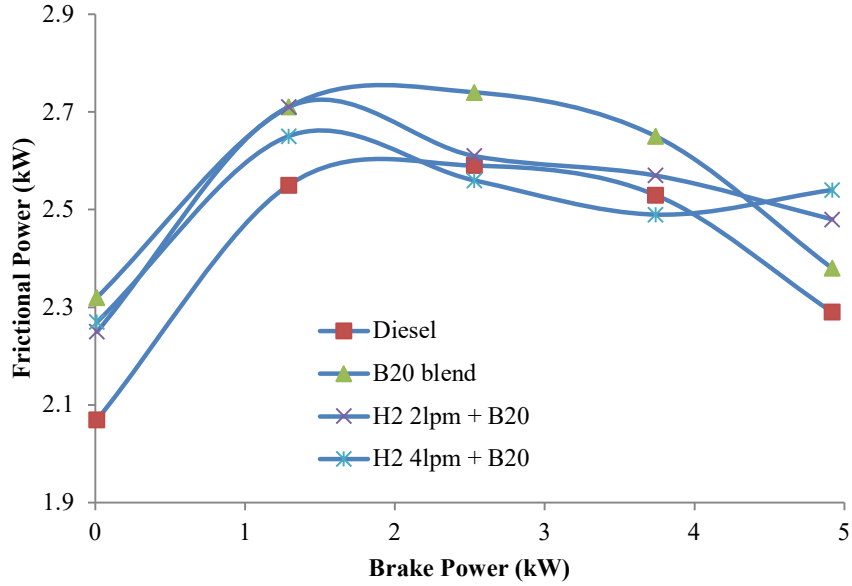

Fig. 6: Variation in Frictional Power.

is high, due to the higher viscosity of the biofuel it is difficult to inject into the chamber which contradicts the combustion rate (Hazar et al. 2022). This is why the friction power decreases when the flow of biodiesel increases at a higher load.

Fig. 7 represents the Brake power (BP) vs Brake thermal efficiency (BTE) of the Engine taken for the analysis. The BTE varies along the Brake power, it shows that the diesel has the highest point at 33.48% at higher load which is 4.92 kW brake power, B20 blend at 30.94%, H_2 at 2 LPM 32.23%, and 4 LPM at 33.6%. Where the hydrogen 4 LPM with B20 blend shows higher BTE with respect to BP due to a higher percentage availability of oxygen present in the biodiesel B20 blend which enhanced the rate of combustion and also with the higher flow rate of hydrogen. It is also to be noted that increasing the ester presence in the fuel will increase the BTE.

Fig. 8 represents Brake power (BP) vs Indicated thermal efficiency (ITE) of the given single cylinder four stroke

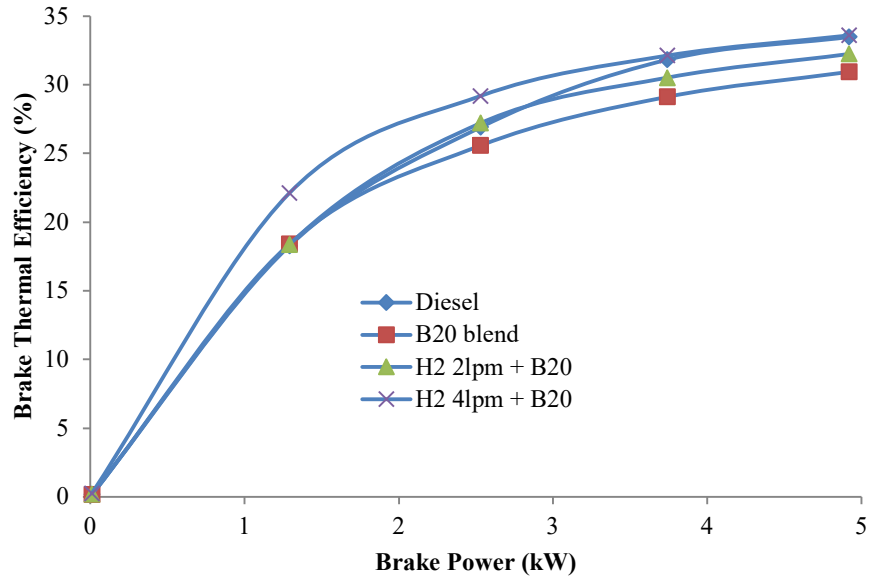

Fig. 7: Variation in Brake Thermal Efficiency.

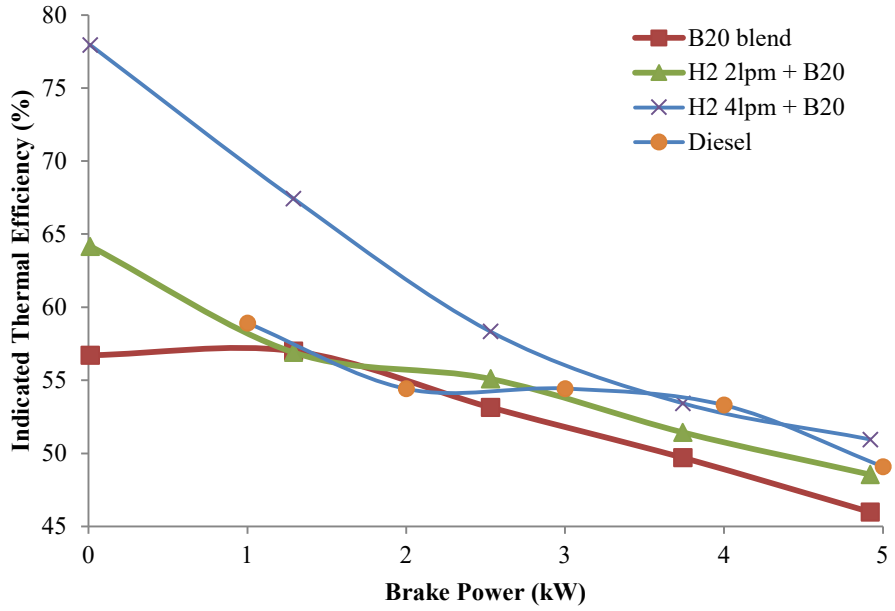

Fig. 8: Variation in Indicated Thermal Efficiency.

diesel Engine. The ITE varies along the B, it shows that the diesel has the highest point at 45.99% at higher load which is 0.01 kW brake power, B20 blend at 48.55 %, H_2 at 2 LPM at 50.95 %, and 4 LPM at 49.09 %. Where the hydrogen 4 LPM with B20 blend shows higher Indicated thermal efficiency with respect to BP due to the higher availability of oxygen present in the biodiesel B20 blend which enhanced the rate of combustion and also with the higher flow rate of hydrogen, and it lowers along the brake power with higher loads and also it is to be noted that heat supplied in the fuel form will influence the indicated thermal efficiency (Zareei et al. 2020).

Fig. 9 represents Brake power vs Specific Fuel Consumption (SFC) of the diesel engine. The SFC varies along the Brake power, it shows that the diesel has the highest point at 0.46 kg/kWh at higher load which is 1.29 kW brake power, B20 blend at 0.47 kg/kWh, H_2 at 2 LPM 0.47 kg/kWh and 4 LPM at 0.39 kg/kWh. Since the

viscosity is higher for the B20 blend, the engine consumes more fuel than the other mixtures, and also due to the lower calorific value of the B20 blend, it needs excess fuel to achieve the expected power output. However, adding H_2 to the fuel mixture decreases the fuel consumption and able the fuel mixture of B20 and H_2 to attain the SFC of diesel fuel. It is to be noted that fuel consumption will increase when the heating value of the fuel decreases, but adding hydrogen in this study has a good influence on SFC.

Fig. 10 represents Brake power vs Total fuel consumption (TFC) of the Diesel Engine. The TFC varies along the BP, it shows that the B20 blend has the highest point at 1.37 kg/hr at Brake power of 4.92 kW, H_2 at 1.32 kg/hr, diesel at 1.25 kg/hr and 4 LPM at 1.26 kg/hr. Where the B20 blend shows higher Total fuel consumption in relation to brake power due to the high viscosity of the B20 blend biofuel which consists of denser molecules that make much volume of fuel and consume a comparatively higher amount of fuel. Because of the viscous nature of the B20 fuel blend, the engine consumes more fuel than the other mixtures, and also due to the lower calorific value of the B20 blend, it is clear that excess fuel is required to produce the expected power output. However, adding H_2 to the fuel mixture decreases the fuel consumption

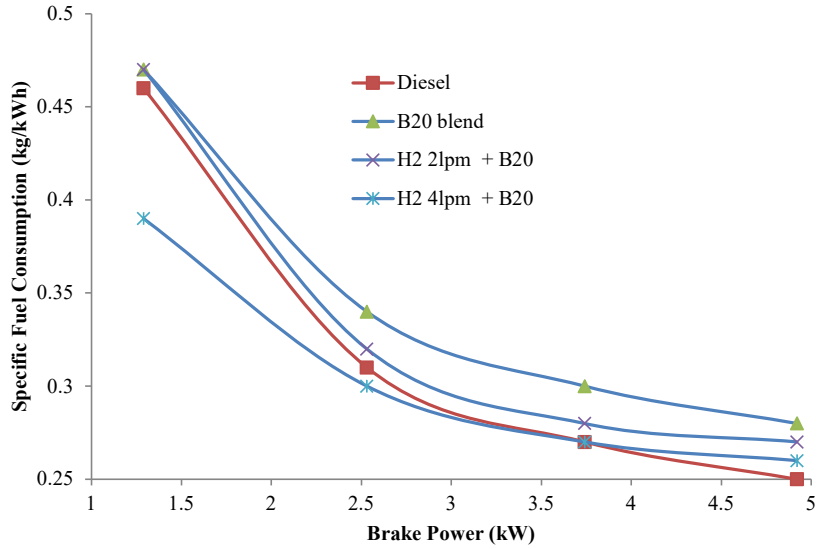

Fig. 9: Variation in Specific Fuel Consumption (SFC).

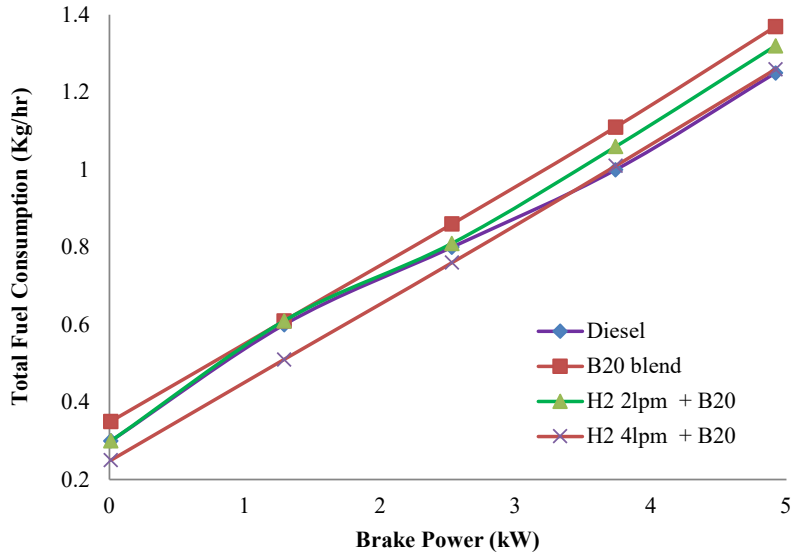

Fig. 10: Variation in Total Fuel Consumption.

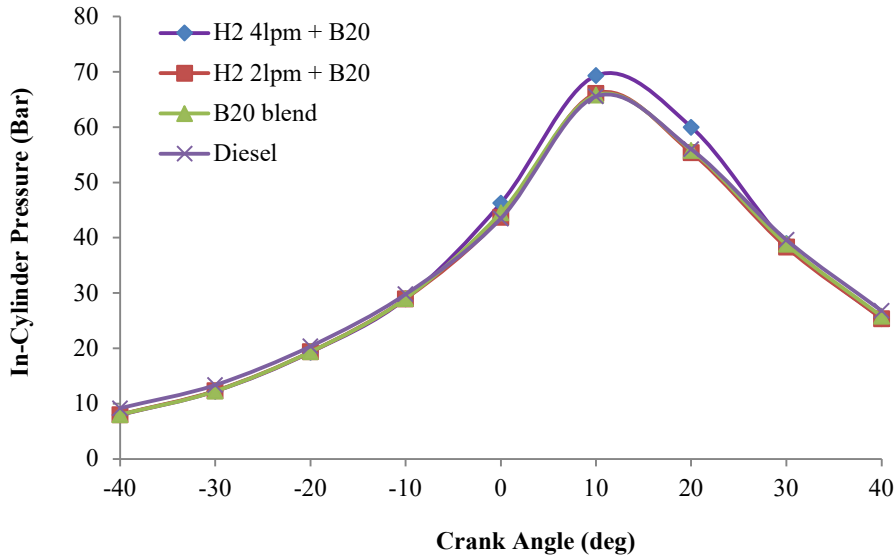

Fig. 11: Variation in in-cylinder pressure.

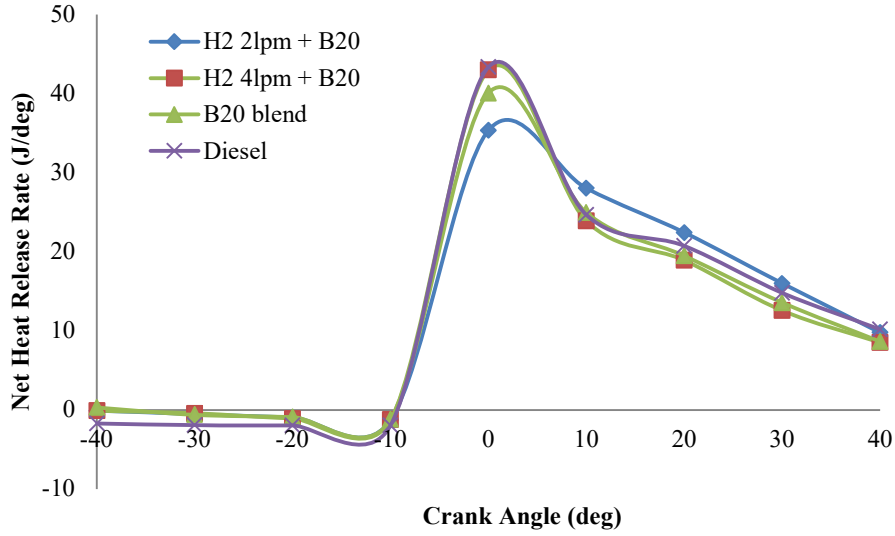

Fig. 12: Variation in Heat Release Rate.

and enables the fuel mixture of B20 and H_2 to attain the TFC of diesel fuel (Avase et al. 2015).

>i g bomni h!>b[l[]n_lcmc]m

This section details about pressure inside the cylinder and rate of heat release representing the combustion characteristics of the *Chlorella vulgaris* biodiesel.

Fig. 11 represents the Crank angle (deg) vs Cylinder pressure of the diesel engine. The cylinder pressure varies along the crank angle. It shows that the H_2 at 4 LPM has the highest point at 69.33 bar at a 10° crank angle, B20 blend at 65.81 bar, diesel at 65.57 bar, and 2 LPM at 66.07 bar. Where the hydrogen 4 LPM with b20 blend shows higher cylinder pressure in relation to crank angle due to the higher flame speed of hydrogen, the B20 blend mixed with hydrogen at 4 LPM shows much increase in the pressure rise rate, in addition, the pressure increased stays a moment and drops down. It is also to be noted that the increase of heat inside the cylinder will affect the pressure of the cylinder (Das et al. 2023).

Fig. 12 represents the Crank angle (deg) vs the Net Heat Release rate of the given diesel Engine. The Net Heat Release rate varies along the crank angle. It shows that the diesel has the highest point at 43.37 J/deg at 0° Crank angle, B20 blend at 40.06 J/deg, H_2 2 LPM at 35.34 J/deg and 4

LPM at 42.98 J/deg. Where diesel shows a higher Net Heat Release rate in relation to crank angle due to high heating value and possessed by its characteristics and lower viscosity compared to biofuel. Even though diesel has the highest heat release rate, hydrogen at 4LPM with B20 blend also shows a similar heat release rate at 0.39 J/deg difference due to the higher calorific value of hydrogen. It is also to be noted that the calorific value and density of the fuel influences widely the heat release rate.

@g cmi h!>b[l[]n_lcmc]m

This section details the characteristics of emission released by the study engine when utilizing the prepared fuel.

Fig. 13 represents Brake power (kW) vs CO (%) of the study engine which is single cylinder four stroke. The CO exhaust varies along the brake power. It shows that the diesel has the highest point at 0.242% at zero loads where brake power is 0.01 kW, B20 blend at 0.087%, H_2 2 LPM + B20 at 0.102% and 4 LPM at 0.196%. Where diesel shows higher CO with respect to brake power because of incomplete combustion of fuel and due to insufficient oxygen compared to biofuel. Because of the enriched oxygen in the biodiesel, it can combust evenly with less amount of CO content emitted

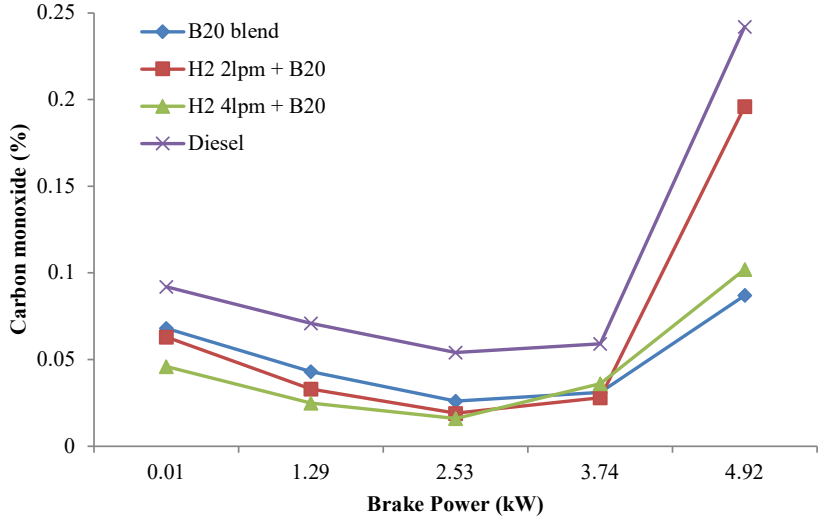

Fig. 13: Variation in CO Emission.

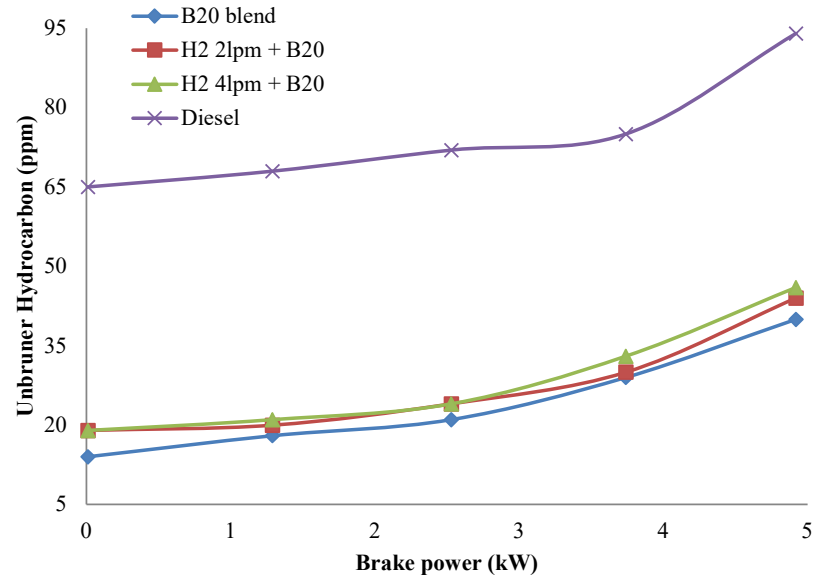

Fig. 14: Variation in Unburned Hydrocarbon Emission.

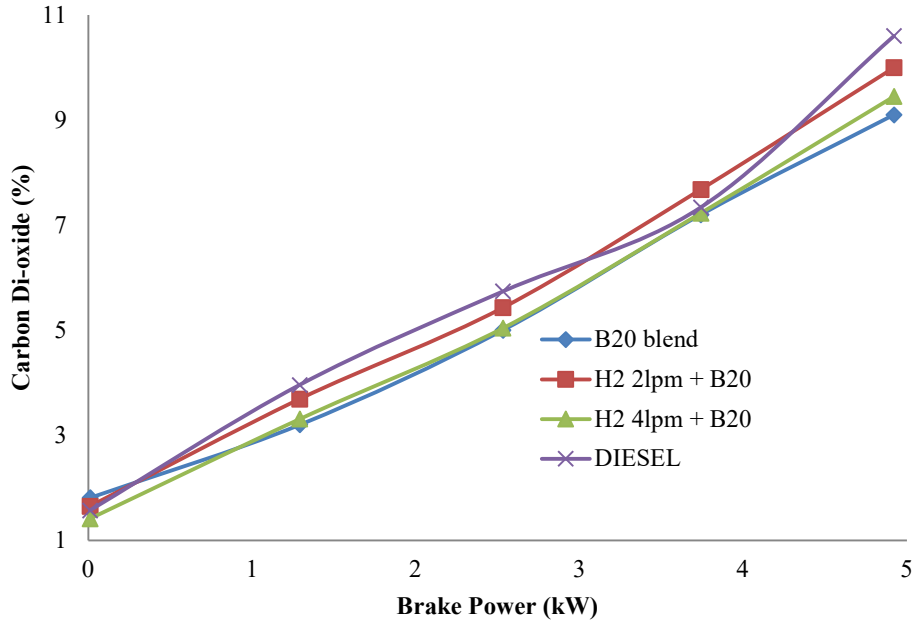

Fig. 15: Variation in CO_2 Emission.

from the B20 blend batch, this case differs when it is added with H_2, this again changes due to less amount of oxygen in the air inlet. This is why the emission of B20 with H_2 is increased compared to the B20 blend (Khan et al. 2018).

Fig. 14 represents Brake power (kW) vs HC (ppm) of the four-stroke diesel engine. The HC exhaust varies along the brake power. It shows that the diesel has the highest point at 94 ppm at zero load where brake power is 0.01 kW, B20 blend at 40 ppm, H_2 2 LPM + B20 at 44 ppm, and 4 LPM at 46 ppm. Due to the high cetane present in the biofuel compared to diesel, it improves the quality of ignition in the fuel and increases the combustion efficiency, and also due to the higher viscosity of the biofuel, there is a delay in ignition of the fuel, this also cause the fuel to burn more even during combustion stroke (Raja et al. 2018). Even though the biodiesel emits less HC, with the addition of H_2, it again increases the Hydrogen content in the exhaust and causes HC to increase.

Fig. 15 represents the Brake power (kW) vs CO_2 (%) of the given diesel Engine. The CO_2 exhaust varies along the BP, it shows that the diesel has the highest point at 10.6% at zero loads where brake power is 0.01 kW, B20 blend at 9.1%, H_2 2 LPM + B20 at 10% and 4 LPM at 9.45%. Where the diesel shows higher CO_2 with respect to brake power because of the combustion of fuel which is incomplete and due to insufficient oxygen compared to biofuel. Because of the enriched oxygen in the biodiesel, it can combust evenly with less amount of CO_2 content emitted from the B20 blend batch, this case differs when it is added with H_2, this again changes due to less amount of oxygen in the air inlet. As a result, the emission of B20 with H_2 was increased compared to the B20 blend (Suzuki et al. 2015).

Fig. 16 represents Brake power (kW) vs NOx ppm of the Engine. The NOx exhaust varies along the brake power. It shows that the B20 + H_2 at 4 LPM has the highest point at 2059 ppm at zero load where brake power is 0.01 kW, B20 blend at 1901 ppm, H_2 2 LPM + B20 at 2002 ppm, and diesel at 1834 ppm. Where diesel shows higher NOx with respect to brake power as a result of incomplete combustion of fuel and because of insufficient oxygen compared to biofuel. Due to the availability of oxygen in the biodiesel, it can combust evenly with less amount of NO_x content emitted from the B20 blend batch, this case differs when it is added with H_2, this again changes due to less amount of oxygen in the air inlet (Oni et al. 2021). Due to this, the emission of B20 with H_2 is increased compared to the B20 blend.

Fig. 17 represents the Brake power (kW) vs O_2 (%) of the Diesel Engine. The O_2 intake varies along the brake power. It shows that the diesel has the highest point at 18.38% at zero load where brake power is 0.01 kW, B20 blend at 18.16%, H_2 2 LPM + B20 at 18.28% and H_2 4 LPM + B20 at 18.3%. Where the diesel shows higher O_2 intake with respect to brake power due to the absence of any kind of supplement air supply and its need to combust the fuel in the combustion chamber.

CONCLUSIONS

An engine that is a single-cylinder four-stroke has been tested at 4 different loads such as 25%, 50%, 75%, and

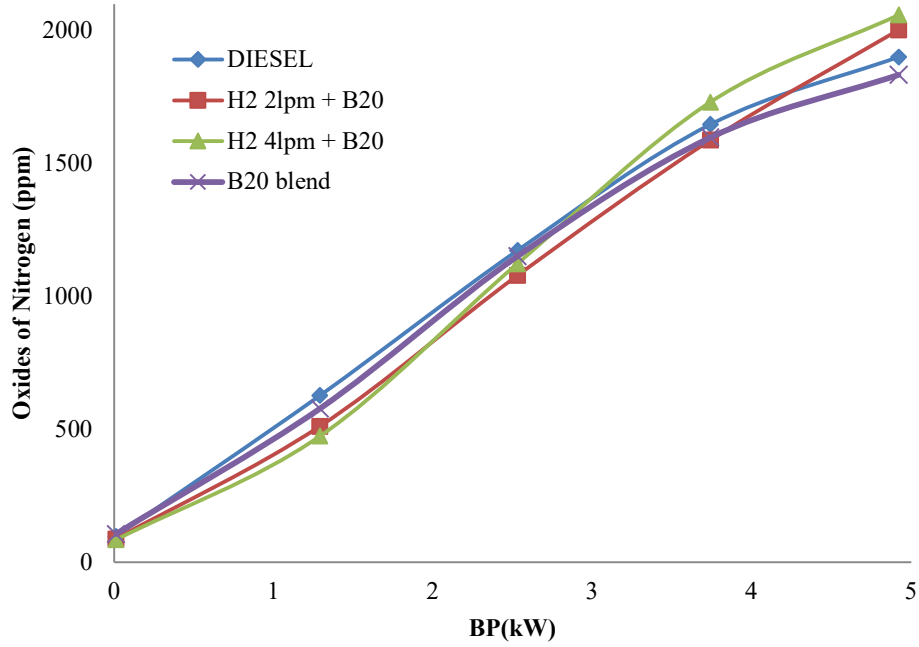

Fig. 16: Variation in NO_x Emission.

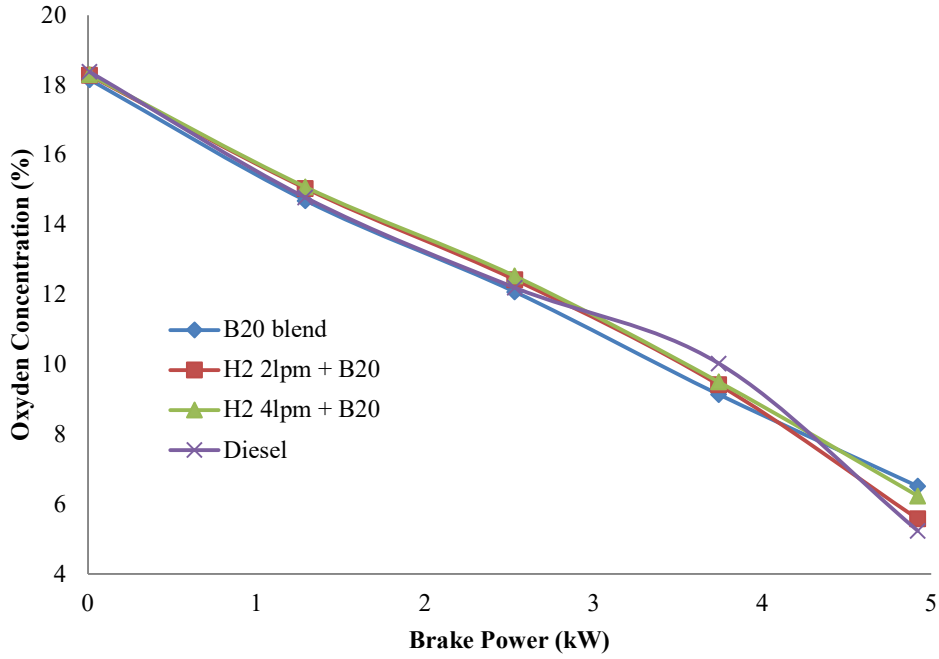

Fig. 17: Variation in O_2 Concentration.

100% load under different hydrogen-biodiesel blend mix ratios. Initially, the engine is tested with a microalgae biodiesel B20 blend and the outputs are observed with various aspects of the engine with such devices as a dynamometer, smoke analyzer, and smoke meter to analyze the performance and emission characteristics of the engine. To observe the combustion traits, there are many flow sensors, temperature, and pressure sensors placed in various inlets and outlets of the combustion chamber. The focal characteristics of the diesel engine such as performance, combustion, and emission are observed and analyzed to conclude.

- B20 blend has higher friction power at 50% load gaining 2.54 kW. Additional O_2 gained from the biodiesel significantly increased the performance of the engine compared to diesel in producing friction power. However, the F.P. reduces at higher loads due to the higher viscosity of the B20 due to which injection of fuel in the combustion chamber becomes difficult which contradicts the combustion property of B20.
- At 100% load, B20 + H_2 at 4 LPM produces higher Brake thermal efficiency, compared to diesel and other fuel mixtures due to an increase in the H_2 flow to the engine. Producing 33.6% BTE at higher loads, comparing Diesel which only produced 33.48% BTE. Though the difference is minimal, the addition of more H_2 to the fuel mixture can produce a significant difference. B20 blend produces only up to 30.94%, so on the whole there is a major difference with increasing H_2.
- Because of the highly viscous nature of the B20 blend, the engine consumes more fuel than the other mixtures, and due to the lower calorific value of the B20 blend, it requires more fuel to produce the expected power output. But adding H_2 to the fuel mixture, decreases the fuel consumption and enables the fuel mixture of B20 and H_2 to attain the SFC of diesel fuel and it also helps in decreasing the total fuel consumption. The specific fuel consumption varies along the Brake power. It shows that the diesel has the highest point at 0.46 kg/kWh at higher load which is 1.29 kW brake power, B20 blend at 0.47 kg/kWh, H_2 at 2 LPM 0.47 kg/kWh, and 4 LPM at 0.39 kg/kWh. BP vs TFC shows that the B20 blend has the highest point at 1.37 kg/hr at brake power of 4.92 kW, H_2 at 1.32 kg/hr, diesel at 1.25 Kg/hr, and 4LPM at 1.26 kg/hr.
- B20 blend + H_2 at 4 LPM mixture has higher indicated power compared to other mixtures, where it is at 7.45 kW due to the high combustible nature of H_2 and due to the availability of a higher amount of oxygen present in the biodiesel, which also helps in increasing the Indicated power of the engine with respect to the brake power produced. With less hydrogen, the I.P. also decreases when compared to diesel which is at 7.22 kW.
- Combustion characteristics show that the cylinder pressure of H_2 at 4 LPM has its highest point at 69.33 bar at a 10° Crank angle, because of the higher flame speed of hydrogen, the B20 blend mixed with hydrogen at 4 LPM shows a significant increase in the rate of pressure rise, in addition, the pressure increased stays a moment and drops down.
- Net Heat Release rate with respect to the Crank angle of H_2 at 4 LPM + B20 produces a higher amount of heat compared to other biofuel mixtures, due to higher calorific value and possessed by its characteristics and lower viscosity compared to biofuel. It shows that the diesel has the highest point at 43.37 J/deg at 0° Crank angle, B20 blend at 40.06 J/deg, H_2 2 LPM at 35.34 J/deg and 4 LPM at 42.98 J/deg. Even though the diesel has the highest Heat release rate, hydrogen at 4 LPM with B20 blend also shows a similar heat release rate at 0.39 J/deg difference due to the higher calorific value of hydrogen.

Comparing other fuel mixtures, the emission of carbon pollutants occurs because of incomplete combustion of fuel in the combustion chamber, but in B20 blend fuel, the fuel combusts more evenly compared to other mixtures. This causes the B20 blend to produce less emission than the mixture with H_2 and conventional fuel.

REFERENCES

Avase, S.A., Srivastava, S., Vishal, K., Ashok, H.V. and Varghese, G., 2015. Effect of pyrogallol as an antioxidant on the performance and emission characteristics of biodiesel derived from waste cooking oil. *Procedia Earth and Planetary Science*, 11, pp.437-444.

Chetia, B., Debbarma, S. and Das, B., 2024. An experimental investigation of hydrogen-enriched and nanoparticle blended waste cooking biodiesel on diesel engine. *International Journal of Hydrogen Energy*, 49, pp.23-37.

Das, S. and Das, B., 2023. The characteristics of waste-cooking palm biodiesel-fueled CRDI diesel engines: effect hydrogen enrichment and nanoparticle addition. *International Journal of Hydrogen Energy*, 48(29), pp.14908-14922.

Godwin John, Hariram, V. and Seralathan, S., 2018. Emission reduction using improved fuel properties of algal oil biodiesel and its blends. *Energy Sources, Part A: Recovery, Utilization, and Environmental Effects*, 40(1), pp.45-53.

Godwin John, Hariram, V., Seralathan, S. and Jaganathan, R., 2017. Effect of Oxygenate on Emission and Performance Parameters of a CI Engine Fuelled with Blends of Diesel-Algal Biodiesel. *International Journal of Renewable Energy Research*, 7(4), pp.2041-2047.

Gultekin, N. and Ciniviz, M., 2023. Experimental investigation of the effect of hydrogen ratio on engine performance and emissions in a compression ignition single cylinder engine with electronically controlled hydrogen-diesel dual fuel system. *International Journal of Hydrogen Energy*, 48(66), pp.25984-25999.

Hariram, V., Godwin John, J. and Seralathan, S., 2017. Spectrometric analysis of algal biodiesel as a fuel derived through base-catalyzed transesterification. *International Journal of Ambient Energy*, 40(2), pp.195-202.

Hariram, V., Prakash, S., Seralathan, S. and Micha Premkumar, T., 2018. Data set on optimized biodiesel production and formulation of emulsified Eucalyptus teriticornisis biodiesel for usage in compression ignition engine. *Data in Brief*, 20, pp.6-13.

Hazar, H., Telceken, T. and Sevinc, H., 2022. An experimental study on emission of a diesel engine fuelled with SME (safflower methyl ester) and diesel fuel. *Energy*, 241, p.122915.

Khan, N., Balunaik, B. and Yousufuddin, S., 2018. Performance and emission characteristics of a diesel engine with varying injection pressure and fueled with hydrogen and cottonseed oil methyl ester blends. *Materials*, 5(2), pp.3369-3377.

Murad, M.E. and Al-Dawody, M.F., 2020. Biodiesel production from spirulina microalgae and its impact on diesel engine characteristics-review. *Al-Qadisiyah Journal for Engineering Sciences*, 13, pp.158-166.

Oni, B.A., Sanni, S.E., Ibegbu, A.J. and Aduojo, A.A., 2021. Experimental optimization of engine performance of a dual-fuel compression-ignition engine operating on hydrogen-compressed natural gas and Moringa biodiesel. *Energy Reports*, 7, pp.607-619.

Raja, S., Mayakrishnan, J., Nandagopal, S., Elumalai, S. and Velmurugan, R., 2018. Comparative study on smoke emission control strategies of a variable compression ratio engine fueled with waste cooking oil. *SAE Technical Paper*, 2018-01-0908.

Rajak, U., Nashine, P., Verma, T.N., Veza, I. and Ağbulut, Ü., 2022. Numerical and experimental investigation of hydrogen enrichment in a dual-fueled CI engine: A detailed combustion, performance, and emission discussion. *International Journal of Hydrogen Energy*, 47(76), pp.32741-32752.

Reang, N.M., Dey, S., Debbarma, B., Deb, M. and Debbarma, J., 2020. Experimental investigation on combustion, performance and emission analysis of 4-stroke single cylinder diesel engine fuelled with neem methyl ester-rice wine alcohol-diesel blend. *Fuel*, 271, p.117602.

Sarpal, A.S., Teixeira, C.M.L.L., Silva, P.R.M., Vieira da Costa Monteiro, T., Itacolomy da Silva, J., Smarcaro da Cunha, V. and Daroda, R.J., 2016. NMR techniques for determination of lipid content in microalgal biomass and their use in monitoring the cultivation with biodiesel potential. *Applied Microbiology and Biotechnology*, 100, pp.2471-2485.

Subramanian, B. and Thangavel, V., 2020. Experimental investigations on performance, emission and combustion characteristics of Diesel-Hydrogen and Diesel-HHO gas in a Dual fuel CI engine. *International Journal of Hydrogen Energy*, 45(46), pp.25479-25492.

Suzuki, Y., Tsujimura, T. and Mita, T., 2015. The performance of multi-cylinder hydrogen/diesel dual fuel engine. *SAE International Journal of Engines*, 8(5), pp.2240-2252.

Tan, D., Wu, Y., Lv, J., Li, J., Ou, X., Meng, Y., Lan, G., Chen, Y. and Zhang, Z., 2023. Performance optimization of a diesel engine fueled with hydrogen/biodiesel with water addition based on the response surface methodology. *Energy*, 263, p.125869.

Zareei, J.A.V.A.D., Haseeb, M., Ghadamkheir, K., Farkhondeh, S.A., Yazdani, A. and Ershov, K., 2020. The effect of hydrogen addition to compressed natural gas on performance and emissions of a DI diesel engine by a numerical study. *International Journal of Hydrogen Energy*, 45(58), pp.34241-34253.